RSC Advances

PAPER

View Article Online
View Journal | View Issue

Cite this: *RSC Adv.*, 2014, **4**, 59519

Effect of air-gap length on carbon dioxide stripping performance of a surface modified polysulfone hollow fiber membrane contactor

M. Rahbari-Sisakht,[ab] F. Korminouri,[a] D. Emadzadeh,[ab] T. Matsuura[c] and A. F. Ismail*[a]

Received 16th September 2014
Accepted 4th November 2014

DOI: 10.1039/c4ra10560e

www.rsc.org/advances

Surface Modifying Macromolecule (SMM) blended PSf hollow fibers were spun at different air-gaps to evaluate CO_2 stripping from aqueous DEA solution and water. The fabricated membranes were firstly subjected to different characterization methods such as contact angle and liquid entry pressure measurement to evaluate the membrane's hydrophobicity and wetting resistance, respectively. To determine pore size and effective porosity of the membranes, a pure helium permeation test was performed. Morphological study of the membranes was conducted by scanning electron microscopy (SEM) and atomic force microscopy (AFM). A CO_2 stripping test was carried out to investigate the effects of operating variables such as liquid and gas velocity, temperature and DEA concentration on the CO_2 stripping flux. It was found that the increase of liquid velocity resulted in enhanced CO_2 stripping flux. On the other hand, the increase in gas velocity did not exert significant influence on the stripping flux. The increase in temperature and DEA concentration both enhanced the stripping flux. Lastly, it was concluded that the hollow fibers spun in this work at a 15 cm air-gap could achieve the best stripping flux among all the membranes fabricated so far for CO_2 stripping.

1. Introduction

Capture and removal of carbon dioxide (CO_2), the main greenhouse gas, from fossil fuel combustion is arguably the most critical environmental concern worldwide. More than 80% of industrial and domestic energy utilization is provided by fossil fuels and they contribute significantly to escalation of atmospheric CO_2 levels, which results inevitably in an increase of significant climate change.[1] A technology for CO_2 removal from gas flows is hence required. Several techniques are presently applied to separate CO_2 from gas streams using various chemical and physical processes including absorption, adsorption, cryogenic and membranes.[2–11] The conventional technologies for CO_2 capture face some operational downsides for instance, flooding, foaming and weeping, which can adversely influence performance and costs of power stations. Hollow fiber membrane (HFM) contactor is an energy and cost efficient technology, which can be applied for depletion of CO_2 from a variety of industrial process gas streams. HFM contactor is a modular and flexible device with a high contact area for liquid and gas phase and high mass transfer rate per unit volume. Due to the noticeable advantages of HFM contactors, in recent years there is an increasing acceptance to use this technology for gas separation.[12–21] The major challenge of using HFs is membrane wettability which results in escalation of mass transfer resistance and reduction of CO_2 flux. To prevent membrane wetting hydrophobic polymers should be chosen.

Polysulfone (PSf) has been used for a long time as a polymeric material for HFM preparation. This polymer, according to Rahbari-Sisakht *et al.*[22] despite not being highly hydrophobic can be a surpassing option for membrane fabrication due to its great thermal and mechanical endurance and high solubility in the solvents. To elevate the hydrophobicity of membrane surface, blending surface modified macromolecules (SMM) in the polymer dope can be a favored method. SMM is an amphipathic macromolecule consisting of hydrophilic and hydrophobic parts. In a polymer blend, thermodynamic incompatibility between polymers usually causes demixing of polymers to occur. If the polymer system is equilibrated in air, the polymer with the lowest surface energy will concentrate at the air interface and reduce the system's interfacial tension as a consequence.[23] In our previous work, EDX results showed that during hollow fiber spinning, SMM tends to migrate to membrane – air surface and changes the membrane outer surface properties.[24] The SMM surface migration occurs during membrane fabrication process due to the difference in energy levels of the SMM and base polymer, which leads to improve hydrophobicity of the HF surface. The detailed kinetics and

[a]*Advanced Membrane Technology Research Center (AMTEC), Universiti Teknologi Malaysia (UTM), 81310 Skudai, Johor, Malaysia. E-mail: afauzi@utm.my; fauzi.ismail@gmail.com; Fax: +60 75535925; Tel: +60 75535592*

[b]*Department of Chemical Engineering, Gachsaran Branch, Islamic Azad University, Gachsaran, Iran*

[c]*Department of Chemical and Biological Engineering, University of Ottawa, 161 Louis Pasteur St., Ontario K1N 6N5, Canada*

mechanism of SMM surface migration is presented in earlier study.[25] The air-gap is one of the principal spinning conditions that affects the amount of migrated SMM to the membrane-interface by providing a sufficient amount of time for SMM migration. The study into the effect of air-gap on membrane performance and structure has been conducted over the past few decades for various separation processes.[26–36]

MC systems have a considerable potential to regenerate or desorb the absorbent solution. In the absorption process, unwanted gas (CO_2) is absorbed by the liquid absorbent. In the regeneration procedure, on the other hand, desorption of CO_2 takes place. The liquid absorbent is in contact with one end of the HFM pore and CO_2 diffuses through the pore, and stripped by the stripping gas at the other end of the pore to regenerate the liquid absorbent.

Many studies have focused on the absorption unit using HFM contactors,[37–39] while only a few works have been carried out until now on CO_2 stripping through MCs. Recently, a research has been done by Khaisri *et al.*[40] to strip CO_2 from monoethanolamine (MEA) solution using polytetrafluoroethylene (PTFE) HFM. They concluded that the stripping efficiency was elevated with the increase of the liquid velocity, operating temperature and absorbent concentration. On the other hand, the gas side mass transfer resistance did not deeply affect the CO_2 desorption flux. Kumazawa[41] conducted a study on CO_2 desorption from 2-amino-2-methyl-1-propanol (AMP) through PTFE membrane. They found that desorption process is ascribed to diffusion and chemical reaction in the liquid side. They concluded that an increase in concentration of AMP and the loaded CO_2 in the solution resulted in enhancement of total mass transfer coefficient. Naim *et al.*[42] produced PVDF membrane to strip CO_2 from aqueous diethanolamine (DEA) solution. They added LiCl in the polymer solution as an additive to investigate the effect of different LiCl levels on stripping performance of the membrane. A linear increase in stripping flux was observed with increasing LiCl concentration. A study by Mansourizadeh and Ismail[43] focused on CO_2 stripping from water using PVDF membrane. Their results showed that the increase of inlet liquid concentration led to increase of CO_2 stripping performance. Rahbari-Sisakht *et al.*[44] fabricated PVDF fibers modified by SMM to strip CO_2 from diethanolamine solution. Their experimental found that the CO_2 desorption flux was enhanced with increasing DEA concentration, solution temperature and liquid velocity. In other works,[45] wet spun polyetherimide (PEI) membrane blended with polyethylene glycol (PEG) was developed to evaluate the effect of various PEI concentrations (13–16 wt%) on CO_2 stripping performance from DEA solution. It was found that the membrane produced with 14 wt% PEI concentration achieved the maximum CO_2 flux of 2.7×10^{-2} (mol m^{-2} s^{-1}).

Despite the above mentioned researches on stripping applications, to our knowledge, no research has been conducted thus far into the effect of SMM migration to the HF membrane surface on CO_2 stripping flux from aqueous DEA solution and water. The first attempt is hence made in the present work to manufacture SMM blended PSf HFs with different air-gap distances, to characterize the HFs so manufactured by various methods and to investigate the performance of CO_2 stripping flux from DEA and water in a MC application.

2. Experimental

2.1. HFM preparation

To prepare spinning dope 17 wt% PSf (Udel P-1700, from Solvay Advance Polymer) and 1 wt% laboratory synthesized SMM was mixed in *N*-methyl-2-pyrrolidone (NMP > 99.5%, purchased from Merck) by mechanical stirring at 60 °C to achieve a stable and uniform solution.

Fig. 1 shows the SMM structure, where *m* represents the repeating units of CF_2 and equals to 7.58, *y* indicates α,ω-aminopropyl poly(dimethyl siloxane) (PDMS) repeating units and is equal to 9.81 and *q* reveals repeating unit of urea and equals to 10.14. The detailed descriptions of SMM synthesis were given in other literatures.[25]

Aqueous solution of diethanolamine (DEA > 99%, from Merck) was used as the liquid absorbent in MC application. The sweeping and feed gas were pure N_2 and CO_2, respectively. After degassing the resulting mixture by the aid of ultrasonic water bath, the PSf HFs (M_1–M_7) were spun with air-gaps of 0, 5, 10, 15, 20, 30 and 50 cm, respectively, according to the method described earlier.[46] Table 1 gives the detailed dry-wet spinning conditions applied in this work. To completely remove the residue of the additive, solvent and any impurities, the spun HFs were soaked in tap water for 3 days, before being dried at room temperature.

2.2. Characterization of prepared HFMs

PSf membranes were subjected to various characterization methods, which meticulously detailed in our previous study.[44] To acquire the average pore radius and the effective surface porosity of the HFs, helium permeation experiment was conducted based on the method described in our earlier work.[44] Contact angle (CA) of the fiber's outer dry surface was measured to obtain information about surface hydrophobicity of the HFs. To determine the membrane's resistance to the wetting, liquid entry pressure for both water (LEPw) and DEA (LEP_{DEA}) was measured.[44] LEPs are considered as the pressure at which the first droplet of liquid was perceived on the upper skin of the HFM. HF's overall porosity (ε_m) was obtained using gravimetric

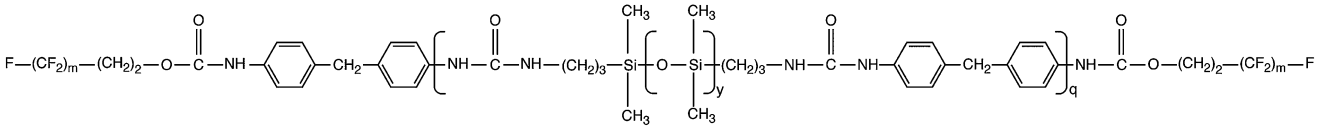

Fig. 1 Structure of SMM.

Table 1 Experimental spinning conditions

Dope extrusion rate (mL min^{-1})	4.5
Composition of bore fluid	NMP/water (60/40)
Bore fluid rate (mL min^{-1})	2.00
Coagulation medium	Tap water
Spinneret dimension, o.d./i.d (mm)	1.20/0.55
Air-gap (cm)	0, 5, 10, 15, 20, 30 and 50
Temperature of coagulant (°C)	25

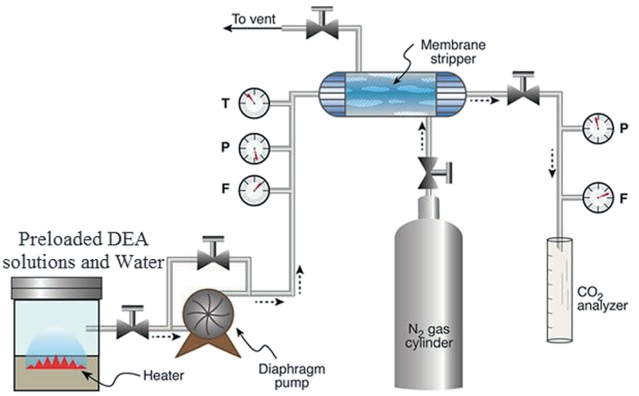

Fig. 2 Experimental apparatus of stripping process *via* MC system.[49]

Table 2 Specifics of MC module

Module i.d (mm)	14
Length of module (mm)	270
HF o.d (μm)	0.7–0.9
HF i.d (μm)	0.45–0.5
Effective length of HF (mm)	150
Number of HFs	30
Effective contact area (inner, mm^2)	6358.5

method. To evaluate HF's mechanical endurance, collapsing pressure of each HF was measured.[44] Scanning electron microscope (SEM, tabletop microscope, TM3000) was used to obtain images of HF's cross-section and outer skin. Roughness (R_a) was obtained by atomic force microscopy (AFM) using AFM equipment (SPA 300 HV, Japan) by the method of Khayet *et al.*[47]

2.3. CO_2 stripping evaluation

Fig. 2 indicates the experimental setup used for CO_2 stripping by the MC system. Thirty HFs were assembled into bundles and placed in a stainless steel module which is specified in details in Table 2. The aqueous DEA solution (1 DEA mol L^{-1}) or water was presaturated with pure CO_2 up to 0.0006 mol L^{-1}, unless otherwise stated, and loaded in the feed reservoir. The CO_2 presaturated liquid and the stripping agent (pure N_2) flowed in the lumen and shell side of HFs, respectively, in a counter flow mode. The calibrated flow meters were applied to regulate the pressure and flow rate of the gas and liquid stream. In order to prohibit the bubble dispersion into the liquid, the difference of 0.2×10^5 bar in pressure between N_2 and the liquid stream was applied. The inlet and outlet CO_2 concentration in the liquid side was determined by the titration method described in details by Li and Chang.[48]

The flux of stripped CO_2 was obtained using the equation below:

$$J_{CO_2} = \frac{C_{l,i} - C_{l,o}}{A_i} \times Q_l \quad (1)$$

where J_{CO_2} is the flux of CO_2 stripped from liquid (mol m^{-2} s^{-1}), $C_{l,i}$ and $C_{l,o}$ indicate concentration of CO_2 (mol m^{-3}) in the liquid stream at the module inlet and outlet, respectively. Q_l is the liquid flow rate (m^3 s^{-1}) and A_i is the HF inner surface (m^2).[49]

3. Results and discussion

3.1. Structure of PSf membranes

The experimental findings of characterization tests are summarized in Table 3. From the table the fiber's mean pore size was very large at the 30 and 50 cm air-gap, which is probably ascribed to elongational effect. As well, the migration of a larger amount of SMM to the fiber surface may also have contributed to pore size enlargement.

The enhancement of contact angle (CA) from 85.14 ± 0.87° to 93.01 ± 0.93° with increasing air-gap up to 15 cm can be attributed to the presence of a larger amount of SMM at the HF surface. On the other hand, a trend of decline in CA from 15 to 50 cm can be attributed to the increased pore size for larger air-gaps. Notably, the increase of the pore size facilitates penetration of water into the HF membrane pores, resulting the reduction in CA values. According to the AFM analysis the roughness of HF outside surface increased as the air gap increased from 0 to 50 cm, which may also have contributed to the enhancement of CA. Further increase in roughness from the air gap of 15 to 50 cm is most likely associated with the increase in pore size, which, as mentioned above has caused the decrease of CA. In any case, all HF surfaces exhibited CA of higher than that of the plain dry spun PSf HF (63 ± 1.5°) by Rahbari-Sisakht *et al.*,[24] which is another evidence of the surface migration of hydrophobic SMM.

The collapsing pressure of PSf HF membranes has gradually increased as the air-gap changed from 0 to 50 cm, which was mainly caused by interaction of base polymer with surface migrated SMM.

The HFs overall porosities are considered to be high enough for MC due to the low polymer concentration in the spinning solution. Furthermore, surprising decrease of The overall porosity decreased gradually with the increase in the air-gap, which is associated with the reduced HF dimension (i.d, o.d and wall thickness) at the higher air-gaps. In addition, a parallel relationship is found between CA and LEPw, *i.e.* both CA and LEPw increased up to 15 cm air-gap, decreased a little from 15 to 20 cm and then increased continuously from 20 to 50 cm. Hence, it can be concluded that LEPw was also influenced by both the pore size and the amount of

Table 3 Experimental data of characterization tests for PSf HFs

HF Number	Air-gap distance (cm)	Average pore size (nm)	Effective surface porosity $\frac{\varepsilon}{L_p}$ (m^{-1})	LEPw ($\times 10^5$ pa)	LEP_{DEA} ($\times 10^5$ pa) at 80 °C	CA (outer surface)	Collapsing pressure ($\times 10^5$ pa)	Overall porosity (%)	Roughness (R_a)
M_1	0	108.95	2.00	5.00 ± 0.72	4.5 ± 0.25	85.14 ± 0.87	7	70	4.12
M_2	5	141.18	1.97	5.00 ± 1.32	4.5 ± 0.68	85.81 ± 1.46	7.5	70	4.85
M_3	10	88.61	3.84	5.00 ± 0.40	4.00 ± 1.40	87.23 ± 1.23	8	69	5.54
M_4	15	21.27	33.28	5.5 ± 0.64	5.00 ± 0.25	93.01 ± 0.93	8.5	68	6.41
M_5	20	62.96	11.40	3.5 ± 1.07	3.00 ± 0.50	88.80 ± 1.37	8.5	68	7.31
M_6	30	257.70	3.10	4 ± 0.82	3.50 ± 1.25	90.00 ± 1.07	9	66	8.06
M_7	50	774.83	0.34	4.5 ± 0.53	3.50 ± 0.50	91.78 ± 1.29	9	58	8.58

Fig. 3 SEM images of the PSF hollow fibers (a) cross-section, (b) outer surface.

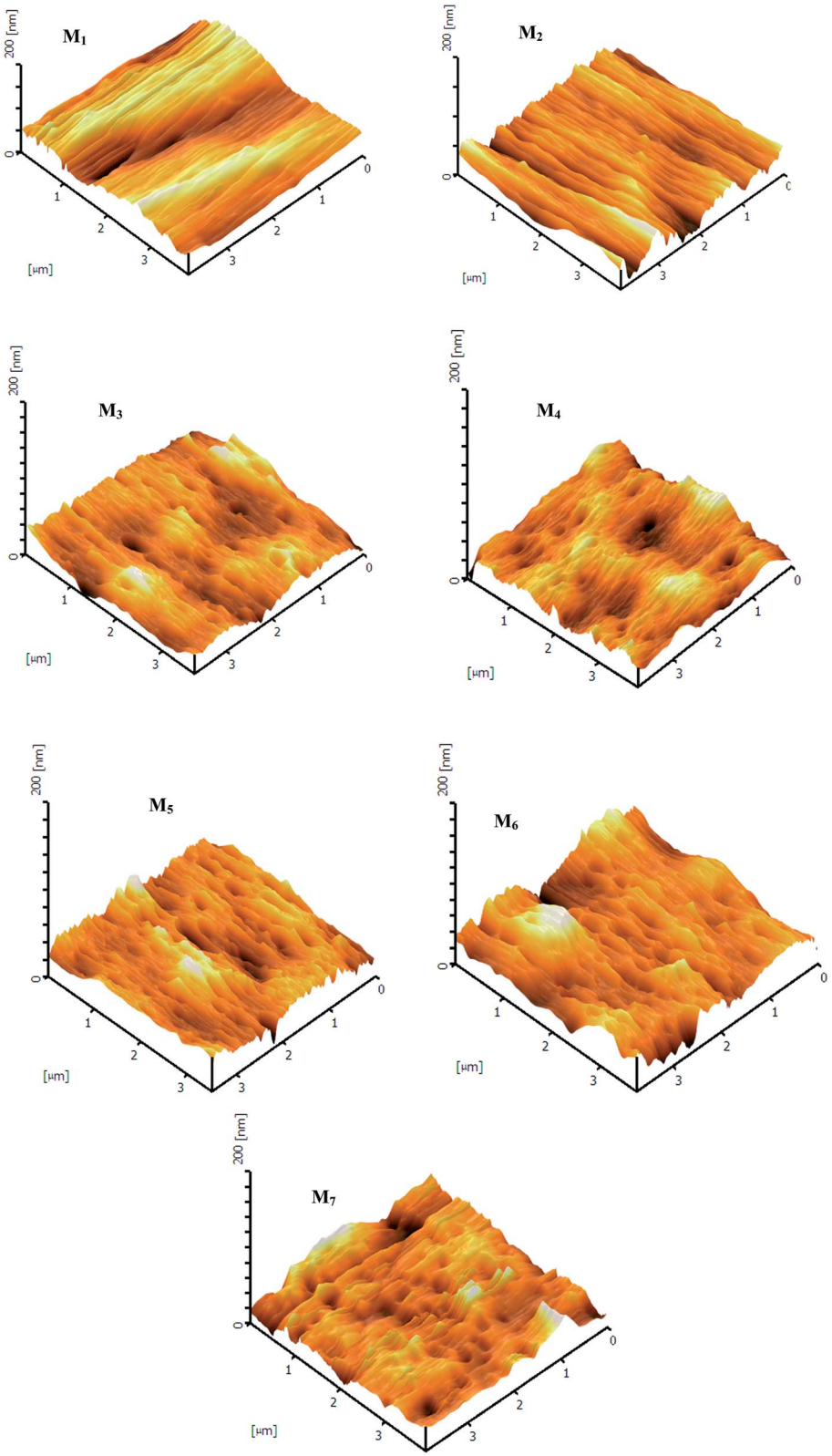

Fig. 4 AFM 3D micrographs of the PSf hollow fibers (outer surface).

migrated SMM to the surface. M_4 membrane showed the highest resistance to the wetting for both water and aqueous DEA solution.

3.2. SEM observation

Fig. 3 displaces the SEM images of the HF's cross-section and the outer skin surface for air-gaps ranging from 0 to 50 cm. The

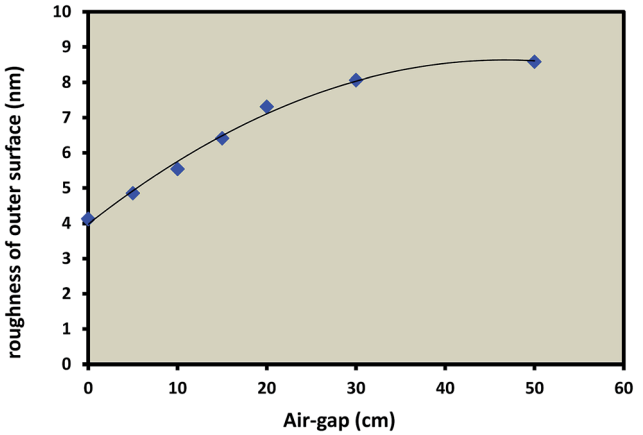

Fig. 5 Roughness parameter of HF's outer surface *vs.* air-gap length.

HF diameters declined from 952 to 654 μm (o.d) and from 604 to 460 μm (i.d), respectively, as the air-gap changed from 0 to 50 cm due to HF elongation. All HFs have porous skin layers on both inner and outer surfaces. Finger-like voids extended from both sides to the middle section of the HF. As shown in Fig. 3 the size of the macrovoids in the HF lumen side became larger as the air-gap length increased, which can be ascribed to the more contact time of the spun HF with the inner coagulant.

3.3. AFM analysis

Fig. 4 shows the 3D AFM micrographs of the HF's outer surface. The roughness of the HF's (M_1–M_7) outer surface increases gradually with an increase in air-gap, as it is quantitatively shown in Fig. 5. The similar morphological behaviour was observed for surface modified polyethersulfone (PES) membranes spun with various air-gaps of 50 to 90 cm, which was attributed to the presence of larger amount of SMM at the HF surface.[50] It is noteworthy that the parallel nodular alignment is obvious for short air-gaps and it becomes more obscure as the air-gap increases. It is likely because of polymer relaxation that occurs while the pristine HF is traveling through the air-gap.

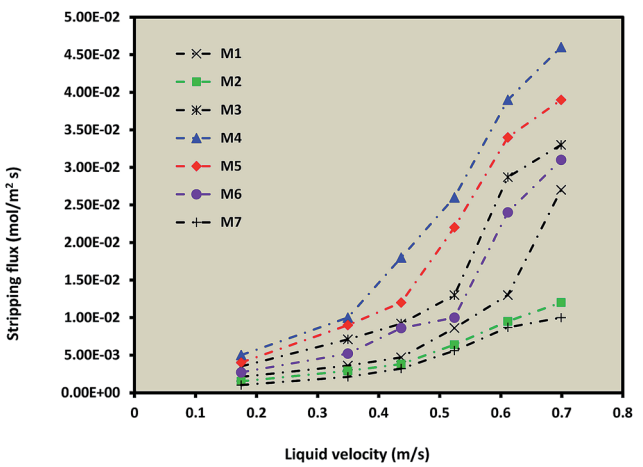

Fig. 6 CO_2 stripping flux *vs.* liquid velocity (DEA solution) ($T_{DEA} = 80$ °C, $M_{DEA} = 1$ mol L^{-1}, gas flow rate = 50 mL min^{-1}).

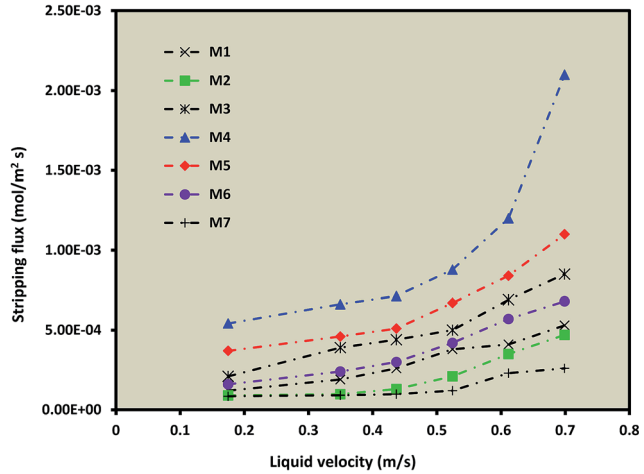

Fig. 7 CO_2 stripping flux *vs.* liquid velocity (water) ($T = 80$ °C, gas flow rate = 50 mL min^{-1}).

3.4. CO_2 stripping evaluation results

Fig. 6 illustrates the influence of liquid (1 mol L^{-1}, DEA) velocity on stripping flux at the liquid temperature of 80 °C. The figure shows an increasing trend in stripping flux as DEA velocity increases, which confirms the decreased resistance of liquid phase boundary layer.[51] A maximum stripping flux of 4.50×10^{-2} (mol m^{-2} s^{-1}) was achieved by HF M_4 at DEA velocity of 0.7 (m s^{-1}). A similar behavior can be seen by Fig. 7 when the liquid absorbent is water.

The membrane that has been fabricated using 15 cm air gap length (M_4) is unique in many aspects among all the studied HFs. In particular, M_4 has the highest effective surface porosity (see Table 3), enabling the fastest gas transport due either to the large surface porosity or to the small effective membrane thickness. Its LEPw is also the highest due to the smallest pore size and the highest contact angle. Thus, M4 has all the desirable features of MC applications.

In Tables 4 and 5 comparisons were made between the CO_2 stripping fluxes from aqueous DEA solution and water, respectively, of the membranes fabricated in this work and those reported in other studies.[44,52–55] The velocity of both DEA solution and water flow was maintained at 0.7 m s^{-1}. As the tables show, M_4 membrane fabricated in this work at 15 cm air-gap and modified with 1 wt% SMM, shows the best CO_2 fluxes.

Fig. 8 demonstrates the relationship between gas velocity and stripping flux for both DEA solution and water. The results for M_4 membrane (15 cm air-gap) are plotted in the figure, but all other HFs would show a similar trend. As shown in Fig. 8, no noticeable stripping flux was perceived as the gas velocity was varied from 0.005 to 0.002 (m s^{-1}). This finding perfectly validates interpretations by Khaisri *et al.* that the liquid phase primarily governs mass transfer rate of MC stripping and the mass transfer resistance of gas stream has negligible effect on stripping flux.[40]

Table 4 Results of CO_2 stripping flux from DEA solution for different HFs

Membrane	Polymer material	Air-gap (cm)	Additive	CO_2 flux (mol m^{-2} s^{-1})	Reference	Liquid absorbent
M_1	PSf	0	1 wt% SMM	2.70×10^{-2}	This work	DEA
M_2	PSf	5	1 wt% SMM	1.20×10^{-2}	This work	DEA
M_3	PSf	10	1 wt% SMM	3.30×10^{-2}	This work	DEA
M_4	PSf	15	1 wt% SMM	4.60×10^{-2}	This work	DEA
M_5	PSf	20	1 wt% SMM	3.90×10^{-2}	This work	DEA
M_6	PSf	30	1 wt% SMM	3.10×10^{-2}	This work	DEA
M_7	PSf	50	1 wt% SMM	1.00×10^{-2}	This work	DEA
—	PVDF	5	1 wt% SMM	1.20×10^{-3}	44	DEA
—	PVDF	0	—	2.20×10^{-2}	55	DEA
—	PVDF	0	5 wt% PEG	3.70×10^{-2}	55	DEA
—	PVDF	0	5 wt% glycerol	2.00×10^{-2}	53	DEA
—	PVDF	0	5 wt% LiCl	3.75×10^{-2}	53	DEA
—	PVDF	0	5 wt% methanol	2.60×10^{-2}	53	DEA
—	PVDF	0	5 wt% phosphoric acid	2.70×10^{-2}	53	DEA
—	PVDF	0	—	2.70×10^{-2}	53	DEA
—	PEI	0	—	9.00×10^{-3}	55	DEA
—	PEI	0	5 wt% PEG	2.35×10^{-2}	55	DEA

Table 5 Results of CO_2 stripping from water for different membranes

Membrane	Polymer material	Air-gap (cm)	Additive	CO_2 flux (mol m^{-2} s^{-1})	Reference	Liquid absorbent
M_1	PSf	0	1 wt% SMM	5.30×10^{-4}	This work	Water
M_2	PSf	5	1 wt% SMM	4.70×10^{-4}	This work	Water
M_3	PSf	10	1 wt% SMM	8.50×10^{-4}	This work	Water
M_4	PSf	15	1 wt% SMM	2.10×10^{-3}	This work	Water
M_5	PSf	20	1 wt% SMM	1.10×10^{-3}	This work	Water
M_6	PSf	30	1 wt% SMM	6.80×10^{-4}	This work	Water
M_7	PSf	50	1 wt% SMM	2.60×10^{-4}	This work	Water
—	PSf	0	4 wt% glycerol	1.30×10^{-4}	54	Water
—	PVDF	0	5 wt% glycerol	1.90×10^{-3}	52	Water

The influence of liquid temperature on the stripping performance of M_4 membrane was also studied and the results for water and DEA solution in Fig. 9 and 10, respectively. As shown in Fig. 9, a marked increase of stripping flux occurred from 2.50×10^{-4} to 4.60×10^{-2} (mol m^{-2} s^{-1}) as the temperature of water changed from 25 °C to 80 °C, which can be attributed to the decrease of CO_2 solubility as the water temperature increases.[44,54] Fig. 10 also shows that the stripping flux of CO_2 increased as the DEA temperature was increased from 25 °C to 80 °C. It could be said that diffusion coefficient, equilibrium constant of chemical reaction and equilibrium partial pressure of CO_2 are strongly influenced by liquid temperature.[40] A decrease in equilibrium constant of the following reaction (eqn (2)) leads to enhancement of CO_2 partial pressure in the gas side by the factor of 5 to 8 as the temperature is increased by 10 °C.[56] Consequently, an increase in working temperature results in elevated driving force for CO_2 stripping from the DEA solution.

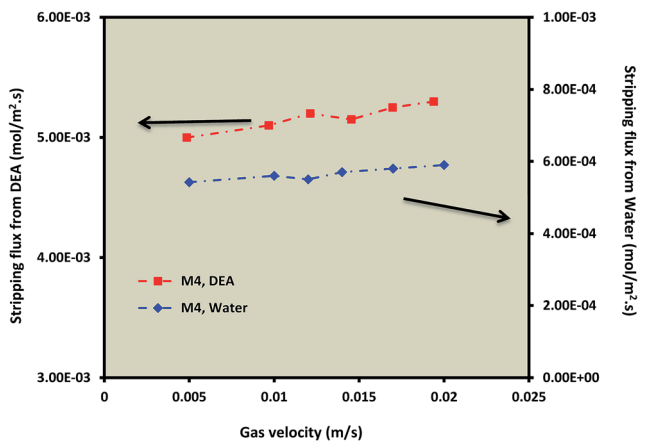

Fig. 8 CO_2 stripping flux *vs.* gas velocity ($T_{DEA\&water} = 80$ °C, $M_{DEA} = 1$ mol L^{-1}, liquid flow rate = 50 mL min^{-1}).

$$CO_2 + 2R_2NH \leftrightarrow R_2NH_2^+ + R_2NCOO^- \quad (2)$$

Fig. 11 reveals the relationship between DEA concentration and stripping flux of M_4 HF in the MC system. As illustrated in the figure an increase in DEA concentration from 0.25 to 1 M results in elevation of stripping flux, which can be validated by the reaction represented by eqn (2). As it is interpreted by Rahbari-Sisakht *et al.*, increase of DEA concentration causes enhancement of absorbed CO_2 during preloading in the form of R_2NCOO^- ion.[44] During the stripping procedure, release of CO_2

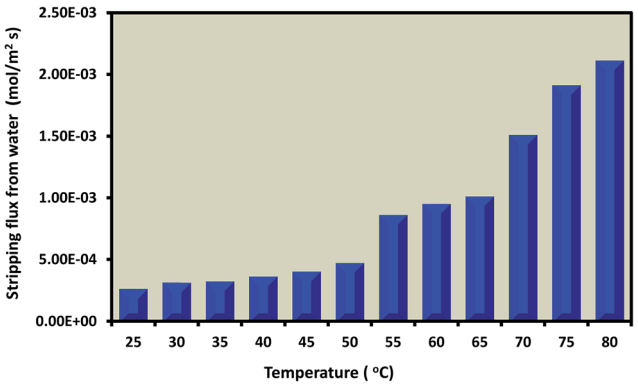

Fig. 9 CO_2 stripping flux *vs.* liquid phase temperature (water) (liquid and gas flow rate = 200, 50 mL min^{-1}, respectively).

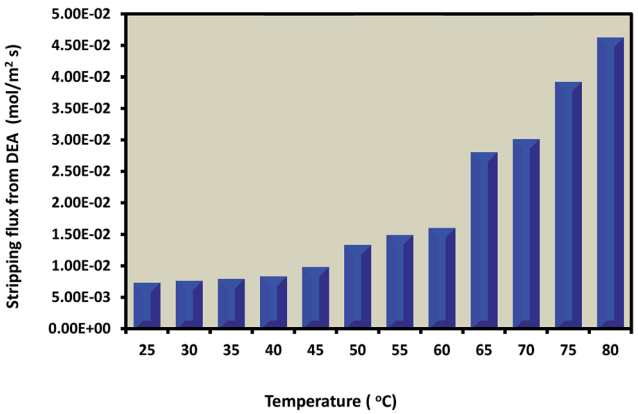

Fig. 10 CO_2 stripping flux *vs.* liquid phase temperature (DEA) (liquid and gas flow rate = 200, 50 mL min^{-1}, respectively).

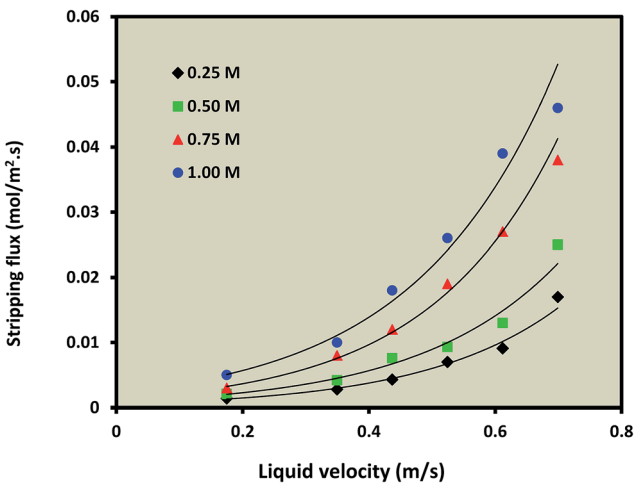

Fig. 11 CO_2 stripping flux *vs.* liquid velocity for various DEA concentration (gas flow rate = 50 mL min^{-1}, T = 80 °C).

causes the elevated CO_2 partial pressure at the interface, resulting in increase of driving force.[40]

4. Conclusion

The SMM blended PSf HFs were spun with air-gaps of 0 to 50 cm and utilized to strip CO_2 by MC from DEA solution and water. M_4 membrane that was spun at 15 cm air-gap showed the highest stripping flux of 4.60×10^{-2} and 2.10×10^{-3} (mol m^{-2} s^{-1}) for DEA solution and water, respectively, at the liquid velocity of 0.7 (m s^{-1}). Higher liquid velocities significantly increased stripping flux; however gas velocity exerted no significant influence, corroborating that liquid boundary resistance is predominant. Additionally, it was found that the change in liquid temperature from 25 °C to 80 °C increased the stripping flux from 2.50×10^{-4} to 2.10×10^{-3} mol m^{-2} s^{-1} and 7.10×10^{-3} to 4.60×10^{-2} mol m^{-2} s^{-1}, for water and DEA solution, respectively. Increasing the DEA concentration from 0.25 to 1 mol L^{-1}, resulted in elevation of stripping flux from 1.70×10^{-2} to 4.60×10^{-2} (mol m^{-2} s^{-1}) at DEA velocity of 0.7 m s^{-1}. Based on the experimental results, the data obtained from the HF spun at the optimum air-gap length (15 cm) surpassed the stripping flux data reported in other studies.

References

1 T. C. Merkel, H. Lin, X. Wei and R. Baker, *J. Membr. Sci.*, 2010, **359**, 126–139.
2 W. J. Koros and G. k. Fleming, *J. Membr. Sci.*, 1993, **83**, 1–80.
3 X. Y. Chen, H. Vinh-Thang, D. Rodrigue and S. Kaliaguine, *RSC Adv.*, 2014, **4**, 12235–12244.
4 S. Danaei Kenarsari, D. Yang, G. Jiang, S. Zhang, J. Wang, A. G. Russell, Q. Wei and M. Fan, *RSC Adv.*, 2013, **3**, 22739–22773.
5 R. W. Baker, *Ind. Eng. Chem. Res.*, 2002, **41**, 1393–1411.
6 J. Lu, L. Wang, X. Sun, J. Li and X. Liu, *Ind. Eng. Chem. Res.*, 2005, **44**, 9230–9238.
7 M. G. Buonomenna, W. Yave and G. Golemme, *RSC Adv.*, 2012, **2**, 10745–10773.
8 D. deMontigny, P. Tontiwachwuthikul and A. Chakma, *Ind. Eng. Chem. Res.*, 2005, **44**, 5726–5732.
9 Z. Wang, M. Fang, H. Yu, C.-C. Wei and Z. Luo, *Ind. Eng. Chem. Res.*, 2013, **52**, 18059–18070.
10 M. S. Abd Rahaman, L. Zhang, L.-H. Cheng, X.-H. Xu and H.-L. Chen, *RSC Adv.*, 2012, **2**, 9165–9172.
11 Y.-F. Lin, C.-C. Ko, C.-H. Chen, K.-L. Tung and K.-S. Chang, *RSC Adv.*, 2014, **4**, 1456–1459.
12 P. H. M. Feron and A. E. Jesen, *Sep. Purif. Technol.*, 2002, **27**, 231–242.
13 V. Y. Dindore, D. W. F. Brilman, P. H. M. Feron and G. F. Versteeg, *J. Membr. Sci.*, 2004, **235**(1–2), 99–109.
14 R. Wang, H. Y. Zhang, P. H. M. Feron and D. T. Liang, *Sep. Purif. Technol.*, 2005, **l46**, 33–40.
15 A. L. Ahmad, A. R. Sunarti, K. T. Lee and W. J. N. Fernando, *Int. J. Greenhouse Gas Control*, 2010, **4**, 495–498.
16 A. Mansourizadeh and A. F. Ismail, *Int. J. Greenhouse Gas Control*, 2011, **5**, 374–380.

17 P. Luis, B. Vander Bruggen and T. Van Gerven, *J. Chem. Technol. Biotechnol.*, 2011, **l86**, 769–775.
18 M. Rahbari-Sisakht, A. F. Ismail, D. Rana and T. Matsuura, *Sep. Purif. Technol.*, 2012, **98**, 472–480.
19 M. Rahbari-Sisakht, A. F. Ismail and T. Matsuura, *Sep. Purif. Technol.*, 2012, **86**, 215–220.
20 A. Mansourizadeh, Z. Aslmahdavi, A. F. Ismail and T. Matsuura, *Int. J. Greenhouse Gas Control*, 2014, **26**, 83–92.
21 M. Rezaei, A. F. Ismail, S. A. Hashemifard, G. Bakeri and T. Matsuura, *Int. J. Greenhouse Gas Control*, 2014, **26**, 147–157.
22 M. Rahbari-sisakht, A. F. Ismail and T. Matsuura, *Sep. Purif. Technol.*, 2012, **88**, 99–106.
23 D. E. Suk, G. Chowdhury, T. Matsuura, R. M. Narbaitz, P. Santerre, G. Pleizier and Y. Deslandes, *Macromolecules*, 2002, **35**, 3017–3021.
24 M. Rahbari-Sisakht, A. F. Ismail, D. Rana and T. Matsuura, *Sep. Purif. Technol.*, 2012, **99**, 61–68.
25 D. E. Suk, T. Matsuura, H. B. Park and Y. M. Lee, *J. Membr. Sci.*, 2006, **277**, 177–185.
26 T. S. Chung and X. Hu, *J. Appl. Polym. Sci.*, 1997, **66**, 1067–1077.
27 D. Wang, K. Li and W. K. Teo, *J. Membr. Sci.*, 1998, **138**, 193–201.
28 D. Wang, K. Li and W. K. Teo, *J. Membr. Sci.*, 1999, **163**, 211–220.
29 D. Wang, K. Li and W. K. Teo, *J. Membr. Sci.*, 2000, **176**, 147–158.
30 J.-J. Qin, J. Gu and T.-S. Chung, *J. Membr. Sci.*, 2001, **182**, 57–75.
31 G. C. Kapantaidakis, G. H. Koops and M. Wessling, *Desalination*, 2002, **144**, 121–125.
32 H. A. Tsai, D. H. Huang, S. C. Fan, Y. C. Wang, C. L. Li and K. R. Lee, *J. Membr. Sci.*, 2002, **198**, 245–258.
33 M. Khayet, *Chem. Eng. Sci.*, 2003, **58**, 3091–3104.
34 K. C. Khulbe, C. Y. Feng, F. Hamad, T. Matsuura and M. Khayet, *J. Membr. Sci.*, 2004, **245**, 191–198.
35 x. Zhang, Y. Wen, Y. Yang and L. Liu, *J. Membr. Sci.*, 2008, **47**, 1039–1046.
36 M. Khayet, M. C. García-Payo, F. A. Qusay and M. A. Zubaidy, *J. Membr. Sci.*, 2009, **330**, 30–39.
37 S.-H. Yeon, K.-S. Lee, B. Sea, Y.-I. Park and K.-H. Lee, *J. Membr. Sci.*, 2005, **257**, 156–160.
38 A. Mansourizadeh, A. F. Ismail, M. S. Abdullah and B. C. Ng, *J. Membr. Sci.*, 2010, **355**, 200–207.
39 H. B. Al-saffar, B. Ozturk and R. Hughes, *Chem. Eng. Res. Des.*, 1997, **75**, 685–692.
40 S. Khaisri, D. deMontigny, P. Tontiwachwuthikul and R. Jiraratananon, *J. Membr. Sci.*, 2011, **376**, 110–118.
41 H. Kumazawa, *Chem. Eng. Commun.*, 2000, **182**, 163–179.
42 R. Naim, A. F. Ismail and A. Mansourizadeh, *J. Membr. Sci.*, 2012, **392–393**, 29–37.
43 A. Mansourizadeh and A. F. Ismail, *Desalination*, 2011, **273**, 386–390.
44 M. Rahbari-Sisakht, A. F. Ismail, D. Rana and T. Matsuura, *J. Membr. Sci.*, 2013, **427**, 270–275.
45 R. Naim and A. F. Ismail, *J. Hazard. Mater.*, 2013, **250–251**, 354–361.
46 A. F. Ismail, I. R. Dunkin, S. L. Gallivan and S. J. Shilton, *Polymer*, 1999, **40**, 6499–6506.
47 M. Khayet, C. Y. K. Feng, C. Khulbe and T. Matsuura, *Desalination*, 2002, **148**, 321–327.
48 M. Li and B.-C. Chang, *J. Chem. Eng. Data*, 1994, **39**, 448–452.
49 M. Rahbari-Sisakht, D. Rana, T. Matsuura, D. Emadzadeh, M. Padaki and A. F. Ismail, *Chem. Eng. J.*, 2014, **246**, 306–310.
50 K. C. Khulbe, C. Y. Feng, T. Matsuura, D. C. Mosqueda-Jimenez, M. Rafat, D. Kingston, R. M. Narbaitz and M. Khayet, *J. Appl. Polym. Sci.*, 2007, **104**, 710–721.
51 M. Simioni, S. E. Kentish and G. W. Stevens, *J. Membr. Sci.*, 2011, **378**, 18–27.
52 A. Mansourizadeh, *Chem. Eng. Res. Des.*, 2012, **90**, 555–562.
53 R. Naim, A. F. Ismail and A. Mansourizadeh, *J. Membr. Sci.*, 2012, **423–424**, 503–513.
54 M. Rahbari-Sisakht, A. F. Ismail, D. Rana, T. Matsuura and D. Emadzadeh, *Sep. Purif. Technol.*, 2013, **108**, 119–123.
55 R. Naim, A. F. Ismail, N. B. Cheer and M. S. Abdullah, *Chem. Eng. Res. Des.*, 2014, **92**, 1391–1398.
56 R. H. Weiland, M. Rawal and R. G. Rice, *AIChE J.*, 1982, **28**, 963–973.